

Tumor-Infiltrating Regulatory T Cells Inhibit Endogenous Cytotoxic T Cell Responses to Lung Adenocarcinoma

Anusha-Preethi Ganesan,^{*,†} Magnus Johansson,^{*} Brian Ruffell,^{*,1} Adam Beltran,^{‡,§} Jonathan Lau,^{*} David M. Jablons,^{*,§} and Lisa M. Coussens^{*,‡,1}

Immune cells comprise a substantial proportion of the tumor mass in human nonsmall cell lung cancers (NSCLC), but the precise composition and significance of this infiltration are unclear. In this study, we examined immune complexity of human NSCLC as well as NSCLC developing in CC10-TAg transgenic mice, and revealed that CD4⁺ T lymphocytes represent the dominant population of CD45⁺ immune cells, and, relative to normal lung tissue, CD4⁺Foxp3⁺ regulatory T cells (T_{regs}) were significantly increased as a proportion of total CD4⁺ cells. To assess the functional significance of increased T_{regs}, we evaluated CD8⁺ T cell-deficient/CC10-TAg mice and revealed that CD8⁺ T cells significantly controlled tumor growth with antitumor activity that was partially repressed by T_{regs}. However, whereas treatment with anti-CD25-depleting mAb as monotherapy preferentially depleted T_{regs} and improved CD8⁺ T cell-mediated control of tumor progression during early tumor development, similar monotherapy was ineffective at later stages. Because mice bearing early NSCLC treated with anti-CD25 mAb exhibited increased tumor cell death associated with infiltration by CD8⁺ T cells expressing elevated levels of granzyme A, granzyme B, perforin, and IFN- γ , we therefore evaluated carboplatin combination therapy resulting in a significantly extended survival beyond that observed with chemotherapy alone, indicating that T_{reg} depletion in combination with cytotoxic therapy may be beneficial as a treatment strategy for advanced NSCLC. *The Journal of Immunology*, 2013, 191: 2009–2017.

Lung cancer is the most common cause of cancer-related mortality worldwide, with ~85% being of the nonsmall cell lung cancer (NSCLC) histological subtype, and associated with prior tobacco use (1). Despite advances in treatment modalities, survival rates for advanced lung cancer remain poor; thus, innovative therapeutic approaches are urgently needed.

Retrospective analysis of most human tumors (2), including lung (3–7), has revealed a significant correlation between immune infiltration by CD8⁺ cytotoxic T cells and improved outcome. In contrast, infiltration of tumors by regulatory T cells (T_{regs}) expressing the lineage-specific transcription factor FOXP3 is instead associated with poor prognosis in NSCLC and other carcinomas

(8–12). As T_{regs} are thought to function primarily in cancer by repressing CD8⁺ T cell functionality, the reciprocal relationship between these two immune cell subtypes indicates that depleting T_{regs} might be therapeutically beneficial.

Indeed, several studies employing carcinogen-induced or transplantable tumor models have reported therapeutic efficacy by depleting T_{regs} based upon increased expression of IL-2R/CD25 (13). However, tumors arise spontaneously following an initiating mutation and not by sudden introduction of fully transformed cells, or by high-dose, short-period carcinogen exposure. Furthermore, therapeutic efficacy in these studies was only observed when depletion was performed prior to tumor cell inoculation or cancer initiation, making translation of these findings to the clinic difficult.

As the tumor immune microenvironment and the immunosuppressive cell types that function in tissues are distinct, we first evaluated leukocyte complexity of human NSCLC and found that CD4⁺ T cells were significantly increased relative to adjacent normal lung tissue, and that CD4⁺FOXP3⁺T_{regs} constituted a significant proportion of these tumor-infiltrating cells. To determine the functional significance of these adaptive leukocytes, and the cellular and molecular mediators of pro- versus antitumor immunity, we used a transgenic mouse model of multistage lung carcinogenesis, namely CC10-TAg mice, in which SV40 T Ag-driven carcinogenesis mirrors that of aggressive human lung cancers (14). We revealed that, whereas CD8⁺ T lymphocytes are critical in restraining lung tumor growth, their recruitment into tumors and bioeffector functions are inhibited by CD4⁺Foxp3⁺T_{regs}, depletion of which significantly prolongs survival of tumor-bearing mice in combination with chemotherapy (CTX).

Materials and Methods

Human tissue samples

Patients with NSCLC who had not received neoadjuvant therapy were recruited into the study under approval of local Institutional Review Boards.

*Department of Pathology, University of California, San Francisco, San Francisco, CA 94143; [†]Cancer Sciences Division, University of Southampton, Southampton SO16 6YD, United Kingdom; [‡]Helen Diller Family Comprehensive Cancer Center, University of California, San Francisco, San Francisco, CA 94143; and [§]Department of Surgery, University of California, San Francisco, San Francisco, CA 94143

¹Current address: Department of Cell and Developmental Biology, Knight Cancer Institute, Oregon Health and Science University, Portland, OR.

Received for publication May 17, 2013. Accepted for publication June 14, 2013.

This work was supported by Cancer Research UK (to A.-P.G.); the Department of Defense Breast Cancer Research Program (to B.R.); National Institutes of Health/National Cancer Institute Grants R01 CA130980, R01 CA140943, R01 CA155331, and U54 CA163123; Department of Defense Breast Cancer Research Program Era of Hope Scholar Expansion Award BC10412; Susan G. Komen Foundation Grants KG111084 and KG110560; the Breast Cancer Research Foundation (to L.M.C.); and National Institutes of Health/National Cancer Institute Grant R01 CA132566 (to D.M.J. and L.M.C.).

Address correspondence and reprint requests to Dr. Lisa M. Coussens at the current address: Cell and Developmental Biology, Knight Cancer Institute, Oregon Health and Science University, Mail Code L215, 3181 SW Sam Jackson Park Road, Portland, OR 97239-3098. E-mail address: coussensl@ohsu.edu

The online version of this article contains supplemental material.

Abbreviations used in this article: CTX, chemotherapy; DC, dendritic cell; NSCLC, nonsmall cell lung cancer; T_{reg}, regulatory T cell.

Copyright © 2013 by The American Association of Immunologists, Inc. 0022-1767/13/\$16.00

Informed written consent was obtained from the patients. Tumor tissue, adjacent normal tissue, and blood were collected from patients following surgical resection at University of California, and histopathological diagnosis was obtained at the same center.

Animal studies

Generation of CC10-TAg mice and characterization of their neoplastic/histopathological stages have been previously reported (15). CC10-TAg mice deficient in B cells (JH^{-/-}), CD4⁺ T cells (CD4^{-/-}), CD8⁺ T cells (CD8^{-/-}), and both CD4⁺ and CD8⁺ T cells (CD4^{+/-}CD8^{+/-}) were generated by backcrossing JH^{+/-}, CD4^{+/-}, CD8^{+/-}, and CD4^{+/-}CD8^{+/-} mice, respectively, into the FvB/n strain to at least N5 (16, 17), followed by intercrossing with CC10-TAg mice. All animal studies and procedures conformed to National Institutes of Health guidelines and were approved by University of California Institutional Animal Care and Use Committee. For in vivo depletion studies, mice were injected i.p. with 400 μg anti-CD25 mAb (clone PC61) and 500 μg anti-CD8 mAb (clone YTS169.4) every 5 d for the respective time periods, as indicated. For survival studies, mice were treated with 400 μg anti-CD25 mAb (clone PC61) or isotype control from 8 wk of age until end stage defined by 15% weight loss. Carboplatin (Hospira) was injected i.p. at 50 mg/kg every 5 d for three doses starting at 13 wk of age.

Histology and tumor size

Mice were sacrificed at indicated time points, and all tissues were collected following intracardiac PBS perfusion. Tissues were fixed in 10% neutral-buffered formalin or frozen in OCT. Tumor burden of each mouse was quantified in five H&E-stained serial sections (100 μm apart) of lungs using Image J software.

Immunohistochemistry

The 5-μm sections of formalin-fixed paraffin-embedded tissues were deparaffinized in xylene and rehydrated by immersion in reducing concentrations of alcohol, followed by PBS. Ag retrieval for CD45, CD8, Foxp3, cleaved caspase-3, and BrdU staining was performed by boiling in citrate buffer (BioGenex), followed by incubation with proteinase K (Dako) for CD31. Endogenous peroxidase activity was quenched by incubation in hydrogen peroxide (Sigma-Aldrich) and methanol at 1:50. Following blocking of nonspecific binding by application of blocking buffer (PBS containing 5% goat serum, 2.5% BSA, and 0.1% Tween 20), tissue sections were incubated overnight with primary Abs, for example, CD8 (Novus Biolabs), Foxp3 (eBioscience), cleaved caspase-3 (Cell Signaling), BrdU (AbD Serotec), CD45 (BD Biosciences), and CD31 (BD Biosciences) at 4°C. After washing in PBS, tissue sections were incubated with their respective biotinylated secondary Abs for 30 min at room temperature, followed by HRP-conjugated avidin complex (ABC Elite; Vector Laboratories). Tissue sections were finally developed with 3,3'-diaminobenzidine (Vector Laboratories), counterstained with methyl green, dehydrated, and mounted with Cytoseal (Thermo Scientific). Slides were digitally scanned by Aperio ScanScope CS Slide Scanner to generate images, and quantification of positive staining was performed using Aperio algorithms.

Flow cytometry

Human and murine lung tissues were sliced and digested using collagenase A (Roche), elastase (Worthington Biochemicals), and DNase (Roche) at 37°C for 20 min. Enzyme activity was quenched by addition of FCS (Sigma-Aldrich), and resulting single-cell suspension was filtered through a 100-μm filter (BD Biosciences). Cells were washed in DMEM (Invitrogen) supplemented with 10% FCS, followed by lysis of erythrocytes (RBCs) by incubation with lysis buffer (BD Biosciences) on ice for 10 min. Live cells were then counted using trypan blue staining with a hemocytometer. Nonspecific Ab binding was blocked by incubation of cells with FcR binding inhibitor (eBioscience) on ice for 30 min, followed by labeling with Fixable Live/Dead Aqua (Invitrogen) and fluorophore-conjugated primary Abs, as has been previously described for humans (18) and mice (19). Cells were washed in PBS containing 1.0% BSA and fixed using BD Cytfix (BD Biosciences) for 30 min, followed by a further wash, and stored at 4°C until analysis. Intracellular staining for Foxp3 was performed using Foxp3 Staining Kit (eBioscience), as per the manufacturer's recommendations. Briefly, following labeling with fluorophore-conjugated primary Abs, cells were fixed using the fixation/permeabilization buffer (eBioscience) and then washed with permeabilization buffer (eBioscience). Cells were incubated with fluorophore-conjugated anti-Foxp3 Ab and further washed using permeabilization buffer

(eBioscience). All samples were analyzed on a LSRII flow cytometer (BD Biosciences).

Quantitative PCR assays

mRNA was obtained by processing tissue samples as per recommendations using RNeasy Micro/Mini Kit (Qiagen) and quantified with NanoDrop ND-1000 (Thermo Fisher Scientific). cDNA was prepared from mRNA by reverse transcription using Superscript III. Preamplification of cDNA for genes of interest was performed using TaqMan PreAmp Master Mix Kit (Applied Biosystems). PCR amplification to 40 cycles was performed using TaqMan gene expression assays (Applied Biosystems) for respective genes and TaqMan gene expression master mix (Applied Biosystems) in 20 μl reactions at recommended cycle temperature conditions on an ABI 7900HT quantitative PCR machine (ABI Biosystems). Differences in gene expression were determined by calculating relative expression as fold change over *TBP* used as the housekeeping gene.

Statistical analyses

Statistical analyses were performed using Prism 4.0 (GraphPad Software). Differences between groups for all parameters were determined using Mann-Whitney *U* test (unpaired, nonparametric, two tailed), except for survival studies in which log rank test was used. **p* < 0.05, ***p* < 0.01, ****p* < 0.001 are shown for all figures.

Results

Human NSCLC are infiltrated by CD4⁺ T and B lymphocytes

Using immunohistochemical and flow cytometric approaches, we evaluated the immune microenvironment within tumors of patients with CTX-naive NSCLC (Supplemental Table I), and found increased presence of CD45⁺ leukocytes within tumors as compared with adjacent normal tissue (Fig. 1A, 1B). Both adaptive lineage (T and B lymphocytes) and innate lineage cells (macrophages, dendritic cells [DCs], and granulocytes) were observed in normal adjacent lung and tumor tissue. However, as compared with adjacent normal lung tissue, the relative composition of leukocytes within tumors was skewed toward higher proportions of CD4⁺ T and B cells (Fig. 1C, 1D). In all of the tumors examined, both CD4⁺ and CD8⁺ T cells displayed activated phenotypes, with most samples displaying higher percentage of CD69⁺ cells in tumors as compared with normal adjacent tissue (Fig. 1E).

Immune complexity of CC10-TAg NSCLC mirrors human NSCLC

CC10-TAg mice express the SV40 large T Ag under control of the Clara cell promoter, and as a consequence develop multifocal pulmonary adenocarcinoma (15) with a gene signature correlated with that of aggressive subtypes of human lung cancers, and thus represent a relevant preclinical model to study NSCLC development (14). In CC10-TAg mice, hyperplastic and dysplastic lung tissue is prominent as early as 4 wk of age, and develops into adenomas by 8 wk, with invasive NSCLC in 100% of mice on the FVB/n strain background between 12 and 16 wk of age (15). Similar to human NSCLC, CC10-TAg tumors are characterized by marked CD45⁺ leukocytic infiltration (Fig. 2A, 2B) with an increased percentage of CD4⁺ T lymphocytes (Fig. 2C, 2D).

Endogenous CD8⁺ cytotoxic T cell responses restrain lung tumor growth in CC10-TAg mice

Because our data indicated that human NSCLC were predominantly infiltrated by activated T lymphocytes, we investigated the functional significance of CD4⁺ T, CD8⁺ T, and B cells in CC10-TAg mice by generating mice harboring homozygous null mutations in genes controlling lineage development. CC10-TAg mice deficient for B220⁺CD19⁺ mature B cells (CC10-TAg/JH^{-/-}), CD4⁺ T cells (CC10-TAg/CD4^{-/-}), CD8⁺ T cells (CC10-TAg/CD8^{-/-}), and mice lacking both CD4⁺ and CD8⁺ T cells (CC10-TAg/CD4^{-/-}CD8^{-/-}) were evaluated for tumor

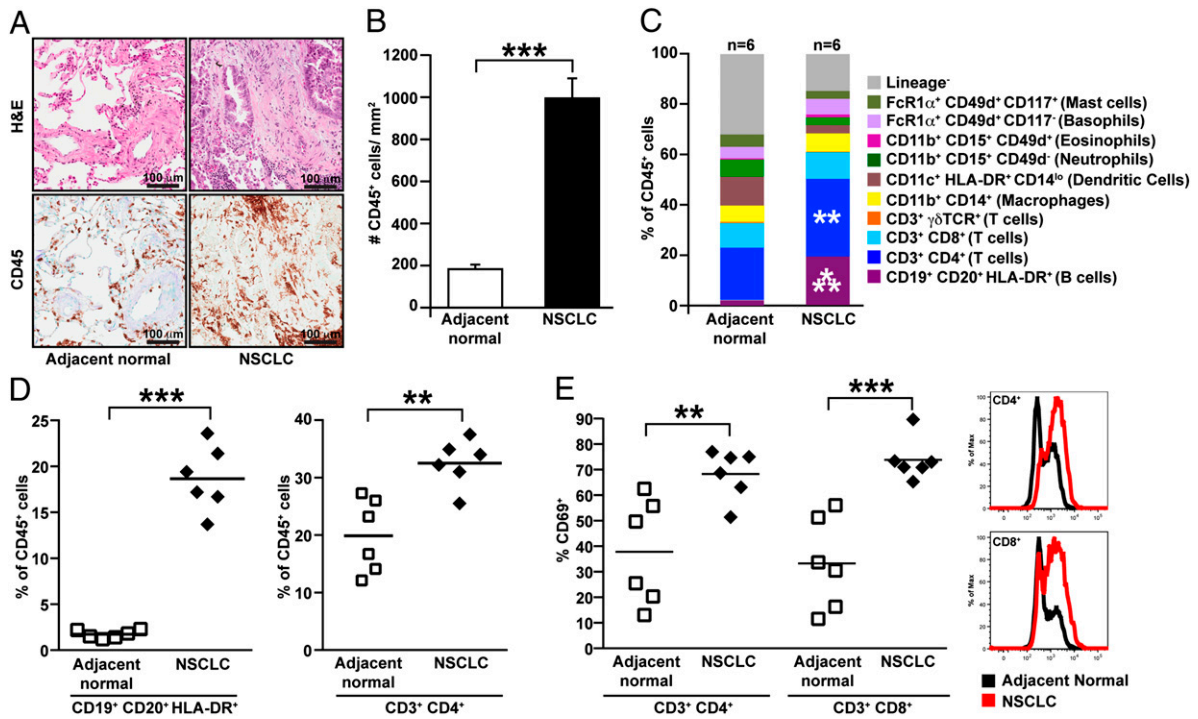


FIGURE 1. Immune complexity of human NSCLC. (A) H&E staining of human NSCLC and adjacent normal tissue (*top panel*) with representative images showing staining for CD45 (*bottom panel*). (B) Numbers of CD45⁺ leukocytes per square millimeter of tissue sections as assessed by immunohistochemistry. *n* = 8 samples per group. (C) Flow cytometric analysis of immune cell infiltrates within human NSCLC represented as percentage of total CD45⁺ leukocytes. *n* = 6 samples per group. (D) CD19⁺CD20⁺HLA-DR⁺ B cell and CD3⁺CD4⁺ T cell infiltrate within human NSCLC, as assessed by flow cytometry, shown as a percentage of total CD45⁺ cells. (E) Percentage of CD4⁺ and CD8⁺ T cells staining positive for CD69, as assessed by flow cytometry, with representative histograms of CD69 expression shown to the *right*. ***p* < 0.01, ****p* < 0.001.

burden at 12 wk of age. CC10-TAg mice lacking CD8⁺ T cells, but not CD4⁺ T cells or B cells, exhibited increased tumor burden (Fig. 3A, 3B), accelerated progression to end stage, and reduced survival (Fig. 3C), indicating that endogenous CD8⁺ T cell responses played a critical role in limiting tumor growth and progression. To demonstrate that the phenotype of CC10-

TAg/CD8^{-/-} mice was not a side effect of genetic manipulation, we depleted CD8⁺ T cells from CC10-TAg mice from 8 to 12 wk of age using anti-CD8–depleting Abs that efficiently depleted CD8⁺ T cells in both spleen and lungs (Supplemental Fig. 1A). Ab-mediated depletion phenocopied the CC10-TAg/CD8^{-/-} mice (Fig. 3D), thereby demonstrating that CD8⁺ T cells were

FIGURE 2. Immune complexity of NSCLC in CC10-TAg mice. (A) H&E staining of lungs from negative littermates (-LM) and CC10-TAg mice showing adenomas and adenocarcinoma (*top panel*), with representative staining for CD45 (*bottom panel*). (B) Numbers of CD45⁺ leukocytes per square millimeter of tissue, as assessed by immunohistochemistry. *n* = 5 mice per group. (C) Flow cytometric analysis of immune cell infiltrates in CC10-TAg lungs assessed at various stages of neoplastic development, namely hyperplasia/dysplasia (4 wk), adenomas (8 wk), and adenocarcinomas (16 wk), represented as percentages of total CD45⁺ leukocytes. (D) CD4⁺ T cell lung infiltrate, as assessed by flow cytometry, shown as a percentage of total CD45⁺ cells. *n* = 5–8 mice per group. Significant differences are shown relative to negative littermates. ***p* < 0.01, ****p* < 0.001.

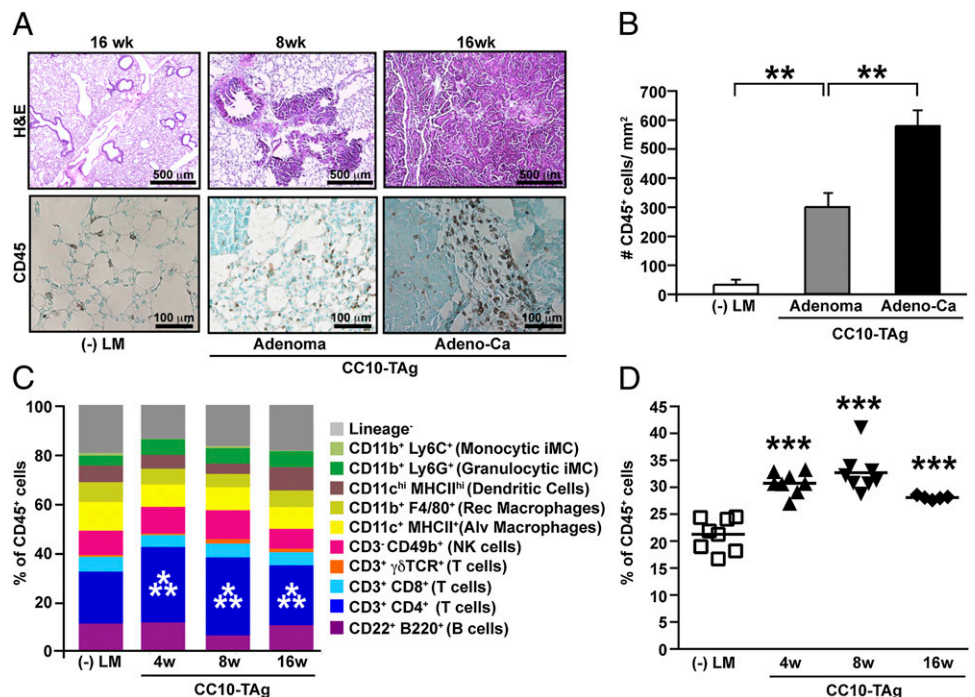
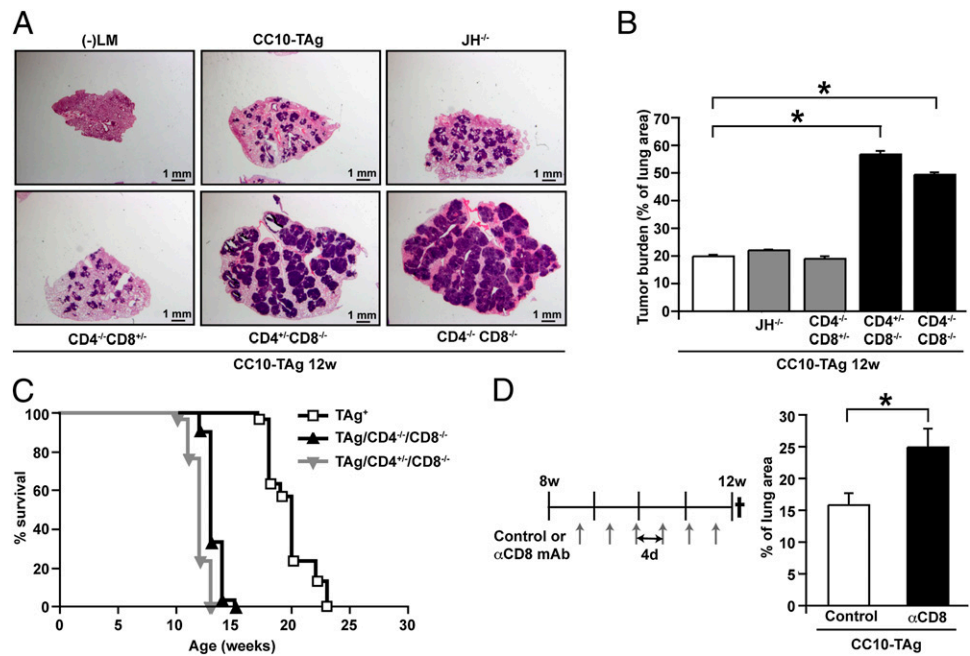


FIGURE 3. CD8⁺ T cells restrain NSCLC growth in CC10-TAg mice. **(A)** H&E staining of lungs from CC10-TAg mice deficient for selective lymphocyte subsets. **(B)** Quantification of tumor burden from mice shown in (A). *n* = 4–5 mice per group. **(C)** Survival of CC10-TAg mice compared with those deficient in CD8⁺ T lymphocytes. *p* < 0.0001; *n* = 30 mice per group. **(D)** Tumor burden quantified as percentage of lung area in CC10-TAg mice following CD8⁺ T cell depletion from 8 wk until 12 wk of age. *n* = 3–7 mice per group, with one of three representative experiments shown. **p* < 0.05.



functionally important in restraining tumor growth in the CC10-TAg model.

Human and CC10-TAg lung tumors are infiltrated by CD4⁺ Foxp3⁺ T_{regs}

CD8⁺ cytotoxic T cells infiltrate lung tumors, where they functionally regulate tumor growth; nevertheless, CC10-TAg tumors continue to progress with mice eventually succumbing to respiratory insufficiency. Given that CD4⁺ T cells abundantly infiltrate tumors relative to nontumor-bearing lungs, we hypothesized that Foxp3⁺ T_{regs} might be enriched within tumors where they functioned to suppress productive CD8⁺ T cell responses. To investigate this, we first ascertained whether T_{regs} were present in tumors by intracellular staining for Foxp3 by flow cytometry and immunohistochemistry. We observed that indeed within human NSCLC tumors (Fig. 4A), there was enrichment of CD4⁺ FOXP3⁺ T_{regs} relative to adjacent normal lung tissue. These findings were mirrored in CC10-TAg lung tumors at multiple stages of tumor development (Fig. 4B), where upregulation of CD103 surface expression in tumor-infiltrating T_{regs}, as compared with normal lungs, was also observed, thus indicating their activated phenotype (Fig. 4C).

T_{reg} depletion diminishes tumor burden in CC10-TAg mice

To examine the functional significance of T_{reg} infiltration of lung tumors, we examined the effects of partial T_{reg} depletion. Although complete and specific elimination of T_{regs} can be achieved by use of scurfy mice (20) harboring a loss-of-function mutation in the Foxp3 gene, or by administration of diphtheria toxin to Foxp3^{DTR} mice (21), development of fatal autoimmunity early on in these mice precludes their use for long-term tumor studies. We thus depleted T_{regs} using an anti-CD25–depleting mAb (clone PC61) that depletes the major subset of Foxp3⁺ T_{regs} expressing CD25, the high-affinity IL-2R α-chain.

Although T_{regs} are characterized by constitutive CD25 expression, CD25 can also be upregulated on conventional CD4⁺ and CD8⁺ T cells following activation. Hence, we first determined the profile of cells expressing CD25 in lung tumors and observed that, within CC10-TAg tumors, the majority of CD25 expressing T cells coexpressed Foxp3 (Supplemental Fig. 1B). Administration of a

single dose of the anti-CD25 mAb resulted in progressive diminution of T_{regs} in peripheral blood, attaining a maximum reduction of 70% as compared with control mice 5 d postinjection, with some evidence of recovery by day 11 (Supplemental Fig. 1C).

Treatment of 4-wk-old CC10-TAg mice every 5 d with anti-CD25 mAb until mice were 8 wk old (Fig. 5D) significantly reduced presence of T_{regs} within spleen and tumor-bearing lungs (Fig. 5E) and led to a significant, albeit minor, reduction in tumor burden (Fig. 5F). This reduction in tumor burden was not due to reduced presence of proliferating malignant lung epithelia (Fig. 4G) or changes in vascular architecture (Fig. 4H), but instead by a marked increased presence of cleaved caspase-3–positive cells (Fig. 4I) that correlated with increased presence of CD8⁺ T cells infiltrating lung parenchyma and tumors (Fig. 4J–L). Together these data indicated that T_{regs} were most likely involved in restricting antitumor activity of tumor-infiltrating CD8⁺ T cells.

Enhanced recruitment of CD8⁺ T cells restricts NSCLC development

Analysis of infiltrating CD8⁺ T cells in T_{reg}-depleted CC10-TAg mice revealed no difference in *in vivo* proliferation as measured by BrdU incorporation (Fig. 5A) or activation as determined by CD69 expression (Fig. 5B). Instead, gene expression analysis of FACS-sorted CD8⁺ T cells isolated from tumors revealed significantly enhanced expression of the Th1 cytokine IFN-γ (Fig. 5C), and cytotoxic effector molecules granzyme A (Fig. 5D), granzyme B (Fig. 5E), and perforin (Fig. 5F). A functional role for CD8⁺ T cells following T_{reg} depletion was confirmed using CC10-TAg/CD8^{-/-} mice, where, as expected, anti-CD25 mAb administration from 4 to 8 wk of age failed to alter tumor burden at end stage (Fig. 5G).

As other studies have reported that T_{reg} suppression of effector T cells may be mediated by cross-talk with APCs (22–25), we also examined whether CD11c⁺MHCII⁺ alveolar macrophage (Supplemental Fig. 2) or CD11c^{high}MHCII^{high} DC (Supplemental Fig. 3) polarization might be altered following partial T_{reg} depletion. Although a significant reduction of CCL17 and CCL22, chemokines known to promote recruitment of T_{regs} into tumors, was observed in tumor-isolated CD11c⁺MHCII⁺ alveolar macrophages, baseline expression of these genes was 100-fold lower

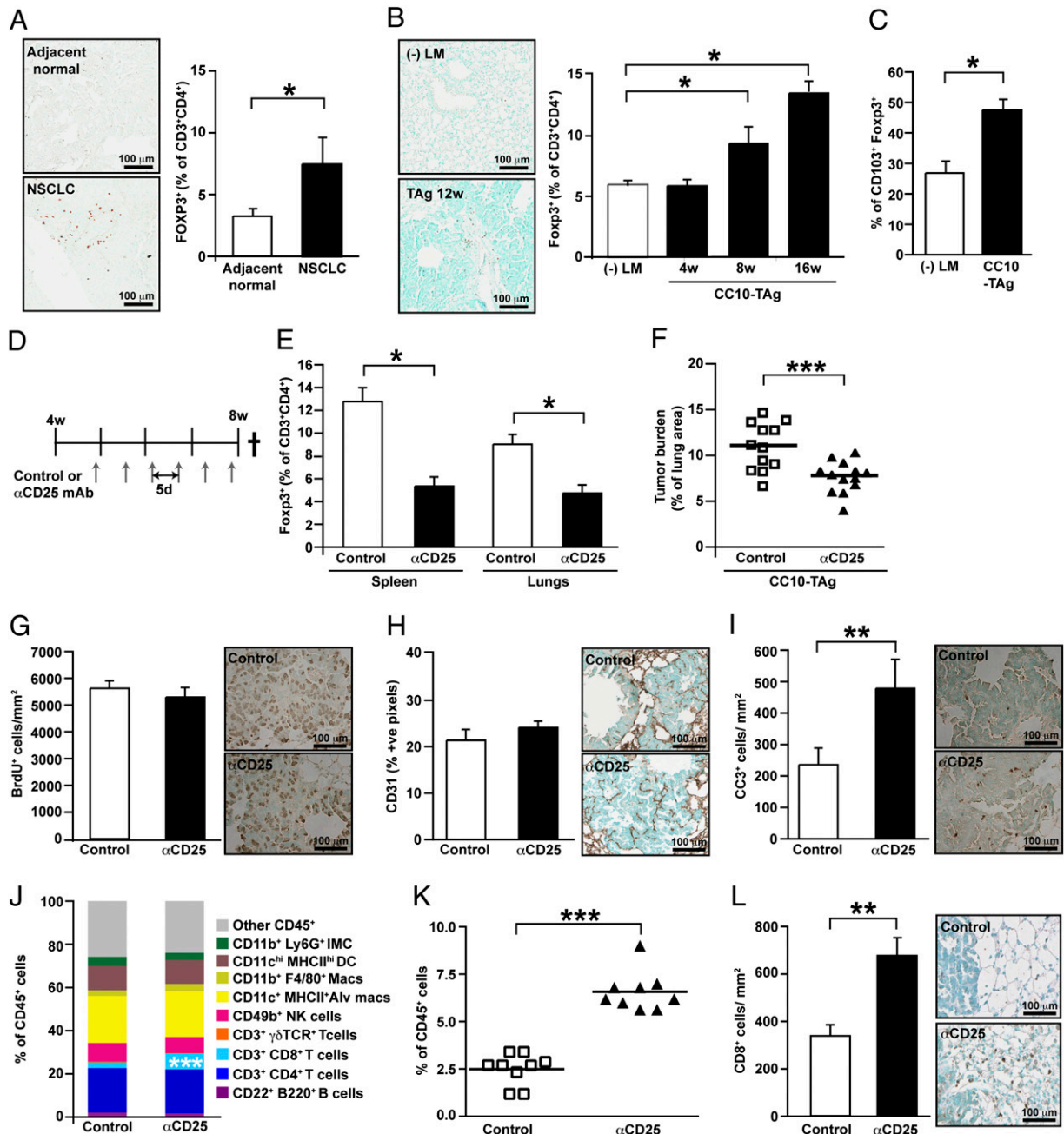


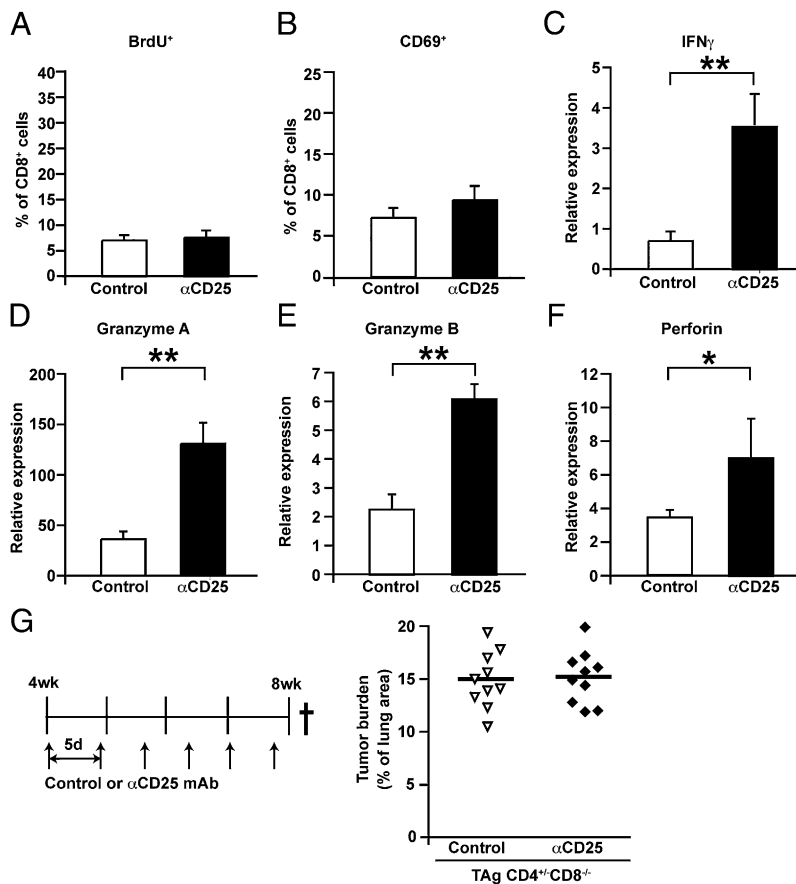
FIGURE 4. Functional significance of T_{regs} in NSCLC. **(A)** Frequency of FOXP3⁺ T_{regs} within the CD4⁺ T cell compartment in human NSCLC assessed by flow cytometry, with representative FOXP3 immunohistochemistry shown on left. *n* = 6 per group. **(B)** Frequency of Foxp3⁺ T_{regs} within the CD4⁺ T cell compartment in CC10-TAG tumors at various ages, as assessed by flow cytometry, with representative Foxp3 immunohistochemistry shown on left. *n* = 5–8 mice per group. **(C)** Percentage of CD3⁺CD4⁺Foxp3⁺ cells expressing CD103⁺ in CC10-TAG tumors. *n* = 5–8 mice per group. **(D)** T_{reg} depletion was assessed in CC10-TAG mice in a prevention trial by i.p. injections of anti-CD25 mAb every 5 d from 4 wk until 8 wk of age. **(E)** Frequency of Foxp3⁺ T_{regs} represented as percentage of CD3⁺CD4⁺ T cells in spleen (left) and lung tumors (right) following treatment with anti-CD25 mAb. **(F)** Tumor burden represented as percentage of lung area following anti-CD25 treatment in CC10-TAG mice. **(G)** Number of BrdU⁺ tumor cells per square millimeter of lung tumors. **(H)** Angiogenic vasculature represented as percentage of positive pixels of CD31 staining by automated quantification of representative stained sections. **(I)** Number of cleaved caspase-3⁺ tumor cells per square millimeter of lung tumors. **(J)** Immune cell complexity of lung tumors following T_{reg} depletion represented as percentage of CD45⁺ leukocytes assessed by flow cytometry. **(K)** CD8⁺ T cell infiltrate of lung tumors, as assessed by flow cytometry, shown as a percentage of total CD45⁺ cells. **(L)** Absolute numbers of CD8⁺ cells per square millimeter of lung tumor with representative immunohistochemistry shown to the right. (E–L) *n* = 12–13 mice per group with data obtained over three independent cohorts of animals. **p* < 0.05, ***p* < 0.01, ****p* < 0.001.

compared with DCs, which did not display altered gene expression. Hence, we reasoned this was unlikely to account for changes in CD8⁺ T cell activity. Based on the modest changes in macrophage and DC transcriptomes, we therefore speculated that T_{regs} were the major leukocyte population repressing CD8⁺ T cell presence and effector function.

T_{reg} depletion in combination with chemotherapy extends survival of CC10-TAG mice

Preclinical studies in murine models of cancer and early-phase clinical trials have revealed limited success in extending survival when immunotherapeutic strategies employing T_{reg} depletion are administered as monotherapy for established tumors (26). Because

FIGURE 5. CD8⁺ T cells in NSCLC following T_{reg} depletion. **(A)** Frequency of BrdU⁺ proliferating CD8⁺ T cells represented as percentages of total tumor-infiltrating CD8⁺ T cells. **(B)** Frequency of CD69-expressing activated CD8⁺ T cells represented as percentages of total tumor-infiltrating CD8⁺ T cells. (A and B) $n = 7$ per group; one of two representative experiments is shown. **(C–F)** Relative expression of *Ifn γ* (C), *Gzma* (D), *Gzmb* (E), and *Prf1* (F) mRNA in flow-sorted CD8⁺ T cells represented as fold change over *Tbp*, as assessed by quantitative PCR. $n = 7$ per group, with data obtained over two independent cohorts of animals. **(G)** Tumor burden represented as percentage of lung area, following treatment with anti-CD25 mAb from 4 wk until 8 wk of age in CC10-TAg mice deficient in CD8⁺ T cells. $n = 10$ per group, with data obtained over three independent cohorts of animals. * $p < 0.05$, ** $p < 0.01$.



T_{reg} depletion attenuated tumor burden in CC10-TAg mice in a prevention trial, we sought to evaluate whether T_{reg} depletion in combination with cytotoxic CTX might extend survival of CC10-TAg mice in a more clinically relevant setting when mice with late-stage NSCLC were treated. Because platinum compounds are first-line standard-of-care chemotherapeutic agents for human NSCLC, we first conducted dose-response experiments with cisplatin in CC10-TAg mice to determine the maximum tolerated dosage that would not produce total leucopenia for use in survival studies. We observed that 50% of CC10-TAg mice did not tolerate administration of both cisplatin and mAb despite the reported safety profile of combinatorial cisplatin and mAbs in clinical trials (27, 28). We therefore conducted a similar dose-response study

with carboplatin, and determined the maximum tolerated dose in combination with anti-CD25 mAb to be 50 mg/Kg, with peripheral blood erythrocytes, leukocytes (lymphocytes and granulocytes), and platelets showing reduced, but not abnormal levels in mice (data not shown).

Thus, CC10-TAg mice were randomized and recruited into four arms to evaluate survival. Mice received control IgG or anti-CD25 mAb as monotherapy from 8 wk of age until end stage (15% weight loss), or received mAbs in combination with carboplatin CTX administered in three doses, 5 d apart, commencing at 13 wk when CC10-TAg mice histopathologically exhibit features of invasive adenocarcinomas. Whereas administration of anti-CD25 mAb as a monotherapy yielded no survival benefit as compared with control

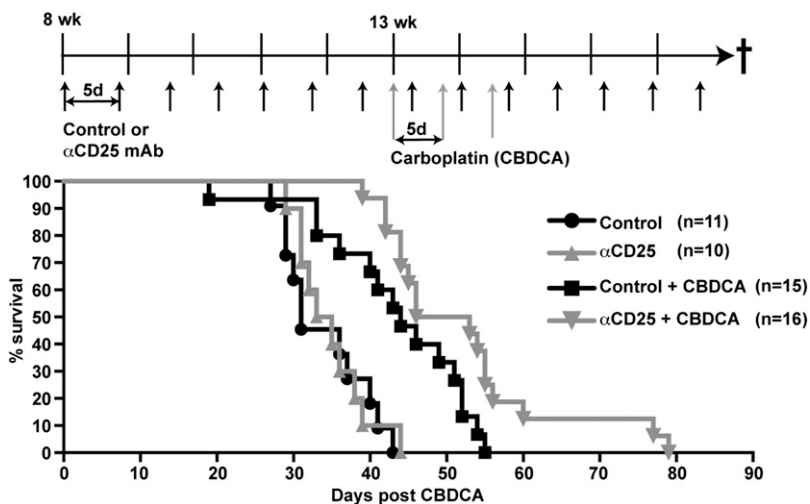


FIGURE 6. T_{reg} depletion in combination with chemotherapy extends survival. Percentage of survival of CC10-TAg mice treated with control IgG or anti-CD25 mAb as monotherapy, or in combination with 50 mg/kg carboplatin (CBDCA). Dosing strategy is shown above the survival graph. Mice received control IgG or anti-CD25 mAb from 8 wk of age until end stage determined by 15% weight loss. Carboplatin was administered in three doses, 5 d apart, commencing at 13 wk. Over 15 cohorts of mice were treated to obtain 10–16 mice per group. $p < 0.05$, control versus CBDCA alone; $p < 0.05$, CBDCA alone versus anti-CD25/CBDCA.

IgG-treated mice, mice that received combination anti-CD25 mAb plus carboplatin exhibited a significant ($p < 0.05$) extension of survival relative to carboplatin alone (Fig. 6).

Discussion

In this study, we evaluated leukocyte complexity of human NSCLC from CTX-naïve patients and in a mouse model of de novo NSCLC development. Results from these studies indicate that, whereas lymphocytes and myeloid cells infiltrate both NSCLC and normal lung, the immune complexity of human NSCLC is dominated by T cells and, in particular, CD4⁺ T and B cells as compared with adjacent normal lung tissue. Interestingly, in over half of the patient tissues examined, both CD4⁺ and CD8⁺ tumor-infiltrating T cells exhibited an activated phenotype based upon expression of CD69, as compared with those in adjacent normal tissue, indicating that these lymphocytes may be functionally significant. CD4⁺ T cells can protect against methylcholanthrene-induced sarcomas (29) and human papillomavirus type 16–induced cervical carcinogenesis (30), whereas other tissues instead promote carcinogen-induced (31) or human papillomavirus type 16–induced squamous cancer (32). In a similar manner, B cells have been found to dampen antitumor immune responses in some murine tumors (33, 34), although augmenting them to enable tumor rejection in others (35, 36). It has therefore become increasingly clear that tumor-infiltrating immune cells exert different bioactivities depending on context, namely tumor etiology and tumor microenvironment.

In CC10-TAg mice harboring NSCLC, neither CD4⁺ T cell nor B cell deficiency significantly altered tumor growth or progression; in contrast, CD8⁺ T cell deficiency led to an acceleration of tumor growth and reduction in survival, thus indicating their critical role in thwarting tumor development in lung. Nevertheless, all CC10-TAg mice succumbed to their disease, indicating tumor immune escape. In keeping with previous reports (37, 38), we found enhanced T cell infiltration in both human and murine NSCLC relative to normal adjacent or nontransgenic lung, respectively. If CD4⁺Foxp3⁺T_{regs} infiltrating NSCLC were functionally significant in promoting tumor immune escape in NSCLC, the expectation would instead be tumor regression in CD4⁺ T cell-deficient CC10-TAg mice, a result that was not observed. However, the conflict in our observation may be accounted for by the simultaneous absence of conventional CD4⁺ T cells in CD4-deficient TAg mice, which may be essential for providing help to CD8⁺ T cells (39, 40).

The functional significance of T_{regs} in several malignancies has been elucidated using mouse models (41–45); however, their precise role in lung cancer is unclear. Furthermore, the in vivo mechanism, the target cell types, and molecular mediators used by T_{regs} to exert their suppressive function in the tumor microenvironment are incompletely understood. In this study, we report that, in CC10-TAg mice, depletion of T_{regs} using the anti-CD25 mAb (PC61) at an early stage of tumor development significantly reduced tumor burden in a manner dependent upon infiltration of functionally active CD8⁺ T cells. Tumor-infiltrating CD8⁺ T cells in T_{reg}-depleted mice did not display enhanced activation or in vivo proliferation, indicating that increased CD8⁺ T cell infiltration observed following T_{reg} depletion was most likely a result of increased recruitment rather than local proliferation. That said, CD8⁺ T cells infiltrating tumors of T_{reg}-depleted mice were characterized by upregulation of effector cytotoxic genes, including granzyme A, granzyme B, and perforin, indicating enhanced functional capacity following release from T_{reg}-mediated suppression. Taken together, these findings indicate that CD8⁺ T cells recruited to NSCLC following T_{reg} depletion were functionally empowered to better kill malignant cells (as indicated by

increased presence of cleaved caspase-3 cells), leading to increased tumor cell death. Our data implicating T_{reg} suppression of CD8⁺ T cells are supported by several studies (41, 42), although other cell types, such as conventional CD4⁺ T cells and NK, have also been reported to be involved (46, 47). Unexpectedly, a recent study by Teng and colleagues revealed a requirement for Th2 cytokines, IL-4 and IL-13, in addition to the Th1 cytokine IFN- γ in achieving tumor control following T_{reg} depletion using restrictive cytokine-deficient mice (48).

T_{regs} regulate APC function as a means of regulating immune responses. T_{regs} establish direct interactions with DCs in lymph nodes, leading to impaired ability to engage and activate T effector cells (49). T_{reg} modulation of macrophages also results in reduced activation, blunted proinflammatory cytokine secretion, upregulation of CD206 and CD163, and reduced macrophage cytotoxicity (50, 51). Both DCs and macrophages can be stimulated by T_{regs} to produce immunosuppressive molecules such as IDO, IL-10, and TGF- β (22, 25, 52). We assessed whether T_{regs} exerted their suppressive effect on APCs in the lung tumor microenvironment and found no significant changes in either DC or macrophage gene expression profiles when comparing cells isolated from T_{reg}-depleted versus control tumor tissue, indicating that T_{regs} most likely directly suppress CD8⁺ T cells in the lung.

Prophylactic T_{reg} depletion in many experimental murine cancer models results in tumor protection when T_{reg} depletion precedes tumor cell implantation (41, 43, 53, 54). In contrast, T_{reg} depletion as monotherapy in large established tumors exhibits minimal impact (26). Recent studies have also revealed that conventional CTX causes tumor regression not just by direct tumor cell killing, but also by eliciting an antitumor cytotoxic immune response (55). Thus, we hypothesized that depletion of T_{regs} in combination with CTX would exert synergistic effects in restraining established tumors. Indeed, we revealed that CC10-TAg mice display enhanced survival when treated with a combination of anti-CD25 mAb and carboplatin, as compared with either treatment alone. This study thus highlights that, even in established tumors, manipulation of T_{regs} may be beneficial in combination with standard-of-care conventional CTX. Survival benefits have also been reported for early treatment of implanted mesothelioma tumors using anti-CD25 mAb and pemetrexed (56). Interestingly, two other reports revealed that complete and selective T_{reg} depletion using DEREK mice controls growth of established implanted tumors in isolation (57) or in combination with vaccination (58). As T_{regs} from transgenic murine tumors have been described to derive from the thymus (59), it will be interesting to determine whether this is also true for implantable tumor models, and whether these cells are functionally equivalent.

Acknowledgments

We acknowledge Drs. David G. DeNardo, Nesrine Affara, Stephen Shiao, and Collin Blakely for helpful discussions, and Lidiya Korets and Kerri Fujikawa for technical assistance with maintenance of animals.

Disclosures

The authors have no financial conflicts of interest.

References

- Jemal, A., F. Bray, M. M. Center, J. Ferlay, E. Ward, and D. Forman. 2011. Global cancer statistics. *CA Cancer J. Clin.* 61: 69–90.
- Fridman, W. H., F. Pagès, C. Sautès-Fridman, and J. Galon. 2012. The immune contexture in human tumours: impact on clinical outcome. *Nat. Rev. Cancer* 12: 298–306.
- Johnson, S. K., K. M. Kerr, A. D. Chapman, M. M. Kennedy, G. King, J. S. Cockburn, and R. R. Jeffrey. 2000. Immune cell infiltrates and prognosis in primary carcinoma of the lung. *Lung Cancer* 27: 27–35.

4. Donnem, T., K. Al-Shibli, S. Andersen, S. Al-Saad, L. T. Busund, and R. M. Bremnes. 2010. Combination of low vascular endothelial growth factor A (VEGF-A)/VEGF receptor 2 expression and high lymphocyte infiltration is a strong and independent favorable prognostic factor in patients with non-small cell lung cancer. *Cancer* 116: 4318–4325.
5. Al-Shibli, K. I., T. Donnem, S. Al-Saad, M. Persson, R. M. Bremnes, and L. T. Busund. 2008. Prognostic effect of epithelial and stromal lymphocyte infiltration in non-small cell lung cancer. *Clin. Cancer Res.* 14: 5220–5227.
6. Welsh, T. J., R. H. Green, D. Richardson, D. A. Waller, K. J. O'Byrne, and P. Bradding. 2005. Macrophage and mast-cell invasion of tumor cell islets confers a marked survival advantage in non-small-cell lung cancer. *J. Clin. Oncol.* 23: 8959–8967.
7. Kawai, O., G. Ishii, K. Kubota, Y. Murata, Y. Naito, T. Mizuno, K. Aokage, N. Saijo, Y. Nishiwaki, A. Gemma, et al. 2008. Predominant infiltration of macrophages and CD8(+) T cells in cancer nests is a significant predictor of survival in stage IV non-small cell lung cancer. *Cancer* 113: 1387–1395.
8. Curiel, T. J., G. Coukos, L. Zou, X. Alvarez, P. Cheng, P. Mottram, M. Evdemon-Hogan, J. R. Conejo-Garcia, L. Zhang, M. Burow, et al. 2004. Specific recruitment of regulatory T cells in ovarian carcinoma fosters immune privilege and predicts reduced survival. *Nat. Med.* 10: 942–949.
9. Bates, G. J., S. B. Fox, C. Han, R. D. Leek, J. F. Garcia, A. L. Harris, and A. H. Banham. 2006. Quantification of regulatory T cells enables the identification of high-risk breast cancer patients and those at risk of late relapse. *J. Clin. Oncol.* 24: 5373–5380.
10. Shen, Z., S. Zhou, Y. Wang, R. L. Li, C. Zhong, C. Liang, and Y. Sun. 2010. Higher intratumoral infiltrated Foxp3+ Treg numbers and Foxp3+/CD8+ ratio are associated with adverse prognosis in resectable gastric cancer. *J. Cancer Res. Clin. Oncol.* 136: 1585–1595.
11. Zhou, J., T. Ding, W. Pan, L. Y. Zhu, L. Li, and L. Zheng. 2009. Increased intratumoral regulatory T cells are related to intratumoral macrophages and poor prognosis in hepatocellular carcinoma patients. *Int. J. Cancer* 125: 1640–1648.
12. Ruffell, B., D. G. DeNardo, N. I. Afara, and L. M. Coussens. 2010. Lymphocytes in cancer development: polarization towards pro-tumor immunity. *Cytokine Growth Factor Rev.* 21: 3–10.
13. Zou, W. 2006. Regulatory T cells, tumour immunity and immunotherapy. *Nat. Rev. Immunol.* 6: 295–307.
14. Deeb, K. K., A. M. Michalowska, C. Y. Yoon, S. M. Krummey, M. J. Hoenerhoff, C. Kavanaugh, M. C. Li, F. J. Demayo, I. Linnoila, C. X. Deng, et al. 2007. Identification of an integrated SV40 T/t-antigen cancer signature in aggressive human breast, prostate, and lung carcinomas with poor prognosis. *Cancer Res.* 67: 8065–8080.
15. Magdaleno, S. M., G. Wang, V. L. Mireles, M. K. Ray, M. J. Finegold, and F. J. DeMayo. 1997. Cyclin-dependent kinase inhibitor expression in pulmonary Clara cells transformed with SV40 large T antigen in transgenic mice. *Cell Growth Differ.* 8: 145–155.
16. de Visser, K. E., L. V. Korets, and L. M. Coussens. 2005. De novo carcinogenesis promoted by chronic inflammation is B lymphocyte dependent. *Cancer Cell* 7: 411–423.
17. Andreu, P., M. Johansson, N. I. Afara, F. Pucci, T. Tan, S. Junankar, L. Korets, J. Lam, D. Tawfik, D. G. DeNardo, et al. 2010. FcRgamma activation regulates inflammation-associated squamous carcinogenesis. *Cancer Cell* 17: 121–134.
18. Ruffell, B., A. Au, H. S. Rugo, L. J. Esserman, E. S. Hwang, and L. M. Coussens. 2012. Leukocyte composition of human breast cancer. *Proc. Natl. Acad. Sci. USA* 109: 2796–2801.
19. DeNardo, D. G., D. J. Brennan, E. Rexhepaj, B. Ruffell, S. L. Shiao, S. F. Madden, W. M. Gallagher, N. Wadhvani, S. D. Keil, S. A. Junaid, et al. 2011. Leukocyte complexity predicts breast cancer survival and functionally regulates response to chemotherapy. *Cancer Discov.* 1: 54–67.
20. Brunkow, M. E., E. W. Jeffery, K. A. Hjerrild, B. Paepfer, L. B. Clark, S. A. Yasayko, J. E. Wilkinson, D. Galas, S. F. Ziegler, and F. Ramsdell. 2001. Disruption of a new forkhead/winged-helix protein, scurf1, results in the fatal lymphoproliferative disorder of the scurfy mouse. *Nat. Genet.* 27: 68–73.
21. Kim, J., K. Lahl, S. Hori, C. Lodenkemper, A. Chaudhry, P. deRoos, A. Rudensky, and T. Sparwasser. 2009. Cutting edge: depletion of Foxp3+ cells leads to induction of autoimmunity by specific ablation of regulatory T cells in genetically targeted mice. *J. Immunol.* 183: 7631–7634.
22. Munn, D. H., and A. L. Mellor. 2004. IDO and tolerance to tumors. *Trends Mol. Med.* 10: 15–18.
23. Mellor, A. L., and D. Munn. 2004. Policing pregnancy: Tregs help keep the peace. *Trends Immunol.* 25: 563–565.
24. Travis, M. A., B. Reizis, A. C. Melton, E. Masteller, Q. Tang, J. M. Proctor, Y. Wang, X. Bernstein, X. Huang, L. F. Reichardt, et al. 2007. Loss of integrin alpha(v)beta8 on dendritic cells causes autoimmunity and colitis in mice. *Nature* 449: 361–365.
25. Coombes, J. L., K. R. Siddiqui, C. V. Arancibia-Carcamo, J. Hall, C. M. Sun, Y. Belkaid, and F. Powrie. 2007. A functionally specialized population of mucosal CD103+ DCs induces Foxp3+ regulatory T cells via a TGF-beta and retinoic acid-dependent mechanism. *J. Exp. Med.* 204: 1757–1764.
26. Quezada, S. A., K. S. Peggs, T. R. Simpson, Y. Shen, D. R. Littman, and J. P. Allison. 2008. Limited tumor infiltration by activated T effector cells restricts the therapeutic activity of regulatory T cell depletion against established melanoma. *J. Exp. Med.* 205: 2125–2138.
27. Pegram, M. D., and D. J. Slamon. 1999. Combination therapy with trastuzumab (Herceptin) and cisplatin for chemoresistant metastatic breast cancer: evidence for receptor-enhanced chemosensitivity. *Semin. Oncol.* 26(Suppl. 12): 89–95.
28. Rosell, R., G. Robinet, A. Szczesna, R. Ramlau, M. Constenla, B. C. Mennequier, W. Pfeifer, K. J. O'Byrne, T. Welte, R. Kolb, et al. 2008. Randomized phase II study of cetuximab plus cisplatin/vinorelbine compared with cisplatin/vinorelbine alone as first-line therapy in EGFR-expressing advanced non-small-cell lung cancer. *Ann. Oncol.* 19: 362–369.
29. Koebel, C. M., W. Vermi, J. B. Swann, N. Zerafa, S. J. Rodig, L. J. Old, M. J. Smyth, and R. D. Schreiber. 2007. Adaptive immunity maintains occult cancer in an equilibrium state. *Nature* 450: 903–907.
30. Daniel, D., C. Chiu, E. Giraud, M. Inoue, L. A. Mizzen, N. R. Chu, and D. Hanahan. 2005. CD4+ T cell-mediated antigen-specific immunotherapy in a mouse model of cervical cancer. *Cancer Res.* 65: 2018–2025.
31. Girardi, M., D. Oppenheim, E. J. Glusac, R. Filler, A. Balmain, R. E. Tigelaar, and A. C. Hayday. 2004. Characterizing the protective component of the alpha beta T cell response to transplantable squamous cell carcinoma. *J. Invest. Dermatol.* 122: 699–706.
32. Daniel, D., N. Meyer-Morse, E. K. Bergsland, K. Dehne, L. M. Coussens, and D. Hanahan. 2003. Immune enhancement of skin carcinogenesis by CD4+ T cells. *J. Exp. Med.* 197: 1017–1028.
33. Shah, S., A. A. Divekar, S. P. Hillechey, H. M. Cho, C. L. Newman, S. U. Shin, H. Nechustan, P. M. Challita-Eid, B. M. Segal, K. H. Yi, and J. D. Rosenblatt. 2005. Increased rejection of primary tumors in mice lacking B cells: inhibition of anti-tumor CTL and TH1 cytokine responses by B cells. *Int. J. Cancer* 117: 574–586.
34. Barbera-Guillem, E., M. B. Nelson, B. Barr, J. K. Nyhus, K. F. May, Jr., L. Feng, and J. W. Sampsel. 2000. B lymphocyte pathology in human colorectal cancer: experimental and clinical therapeutic effects of partial B cell depletion. *Cancer Immunol. Immunother.* 48: 541–549.
35. Schultz, K. R., J. P. Klarinet, R. S. Gieni, K. T. HayGlass, and P. D. Greenberg. 1990. The role of B cells for in vivo T cell responses to a Friend virus-induced leukemia. *Science* 249: 921–923.
36. DiLillo, D. J., K. Yanaba, and T. F. Tedder. 2010. B cells are required for optimal CD4+ and CD8+ T cell tumor immunity: therapeutic B cell depletion enhances B16 melanoma growth in mice. *J. Immunol.* 184: 4006–4016.
37. Schneider, T., S. Kimpfler, A. Warth, P. A. Schnabel, H. Dienemann, D. Schadendorf, H. Hoffmann, and V. Umansky. 2011. Foxp3(+) regulatory T cells and natural killer cells distinctly infiltrate primary tumors and draining lymph nodes in pulmonary adenocarcinoma. *J. Thorac. Oncol.* 6: 432–438.
38. Dimitrakopoulos, F. I., H. Papadaki, A. G. Antonacopoulou, A. Kottorou, A. D. Gotsis, C. Scopu, H. P. Kalofonos, and A. Mouzaki. 2011. Association of FOXP3 expression with non-small cell lung cancer. *Anticancer Res.* 31: 1677–1683.
39. Sun, J. C., M. A. Williams, and M. J. Bevan. 2004. CD4+ T cells are required for the maintenance, not programming, of memory CD8+ T cells after acute infection. *Nat. Immunol.* 5: 927–933.
40. Shedlock, D. J., and H. Shen. 2003. Requirement for CD4 T cell help in generating functional CD8 T cell memory. *Science* 300: 337–339.
41. Onizuka, S., I. Tawara, J. Shimizu, S. Sakaguchi, T. Fujita, and E. Nakayama. 1999. Tumor rejection by in vivo administration of anti-CD25 (interleukin-2 receptor alpha) monoclonal antibody. *Cancer Res.* 59: 3128–3133.
42. Shimizu, J., S. Yamazaki, and S. Sakaguchi. 1999. Induction of tumor immunity by removing CD25+CD4+ T cells: a common basis between tumor immunity and autoimmunity. *J. Immunol.* 163: 5211–5218.
43. Golgher, D., E. Jones, F. Powrie, T. Elliott, and A. Gallimore. 2002. Depletion of CD25+ regulatory cells uncovers immune responses to shared murine tumor rejection antigens. *Eur. J. Immunol.* 32: 3267–3275.
44. Casares, N., L. Arrillaga, P. Sarobe, J. Dotor, A. Lopez-Diaz de Cerio, I. Melero, J. Prieto, F. Borrás-Cuesta, and J. Lasarte. 2003. CD4+/CD25+ regulatory cells inhibit activation of tumor-primed CD4+ T cells with IFN-gamma-dependent antiangiogenic activity, as well as long-lasting tumor immunity elicited by peptide vaccination. *J. Immunol.* 171: 5931–5939.
45. Jones, E., M. Dahm-Vicker, A. K. Simon, A. Green, F. Powrie, V. Cerundolo, and A. Gallimore. 2002. Depletion of CD25+ regulatory cells results in suppression of melanoma growth and induction of autoreactivity in mice. *Cancer Immun.* 2: 1.
46. Beyer, M., and J. L. Schultze. 2006. Regulatory T cells in cancer. *Blood* 108: 804–811.
47. Ghiringhelli, F., C. Ménard, M. Terme, C. Flament, J. Taieb, N. Chaput, P. E. Puig, S. Novault, B. Escudier, E. Vivier, et al. 2005. CD4+CD25+ regulatory T cells inhibit natural killer cell functions in a transforming growth factor-beta-dependent manner. *J. Exp. Med.* 202: 1075–1085.
48. Teng, M. W., J. B. Swann, B. von Scheidt, J. Sharkey, N. Zerafa, N. McLaughlin, T. Yamaguchi, S. Sakaguchi, P. K. Darcy, and M. J. Smyth. 2010. Multiple antitumor mechanisms downstream of prophylactic regulatory T-cell depletion. *Cancer Res.* 70: 2665–2674.
49. Tadokoro, C. E., G. Shakhbar, S. Shen, Y. Ding, A. C. Lino, A. Maraver, J. J. Lafaille, and M. L. Dustin. 2006. Regulatory T cells inhibit stable contacts between CD4+ T cells and dendritic cells in vivo. *J. Exp. Med.* 203: 505–511.
50. Mahajan, D., Y. Wang, X. Qin, Y. Wang, G. Zheng, Y. M. Wang, S. I. Alexander, and D. C. Harris. 2006. CD4+CD25+ regulatory T cells protect against injury in an innate murine model of chronic kidney disease. *J. Am. Soc. Nephrol.* 17: 2731–2741.
51. Tiemessen, M. M., A. L. Jagger, H. G. Evans, M. J. van Herwijnen, S. John, and L. S. Taams. 2007. CD4+CD25+Foxp3+ regulatory T cells induce alternative activation of human monocytes/macrophages. *Proc. Natl. Acad. Sci. USA* 104: 19446–19451.
52. Zhen, Y., J. Zheng, and Y. Zhao. 2008. Regulatory CD4+CD25+ T cells and macrophages: communication between two regulators of effector T cells. *Inflamm. Res.* 57: 564–570.
53. Tawara, I., Y. Take, A. Uenaka, Y. Noguchi, and E. Nakayama. 2002. Sequential involvement of two distinct CD4+ regulatory T cells during the course of

- transplantable tumor growth and protection from 3-methylcholanthrene-induced tumorigenesis by CD25-depletion. *Jpn. J. Cancer Res.* 93: 911–916.
54. Yu, P., Y. Lee, W. Liu, T. Krausz, A. Chong, H. Schreiber, and Y. X. Fu. 2005. Intratumor depletion of CD4+ cells unmasks tumor immunogenicity leading to the rejection of late-stage tumors. *J. Exp. Med.* 201: 779–791.
55. Zitvogel, L., L. Apetoh, F. Ghiringhelli, and G. Kroemer. 2008. Immunological aspects of cancer chemotherapy. *Nat. Rev. Immunol.* 8: 59–73.
56. Anraku, M., T. Tagawa, L. Wu, Z. Yun, S. Keshavjee, L. Zhang, M. R. Johnston, and M. de Perrot. 2010. Synergistic antitumor effects of regulatory T cell blockade combined with pemetrexed in murine malignant mesothelioma. *J. Immunol.* 185: 956–966.
57. Teng, M. W., S. F. Ngiew, B. von Scheidt, N. McLaughlin, T. Sparwasser, and M. J. Smyth. 2010. Conditional regulatory T-cell depletion releases adaptive immunity preventing carcinogenesis and suppressing established tumor growth. *Cancer Res.* 70: 7800–7809.
58. Klages, K., C. T. Mayer, K. Lahl, C. Loddenkemper, M. W. Teng, S. F. Ngiew, M. J. Smyth, A. Hamann, J. Huehn, and T. Sparwasser. 2010. Selective depletion of Foxp3+ regulatory T cells improves effective therapeutic vaccination against established melanoma. *Cancer Res.* 70: 7788–7799.
59. Malchow, S., D. S. Leventhal, S. Nishi, B. I. Fischer, L. Shen, G. P. Paner, A. S. Amit, C. Kang, J. E. Geddes, J. P. Allison, et al. 2013. Aire-dependent thymic development of tumor-associated regulatory T cells. *Science* 339: 1219–1224.